INTERNATIONAL JOURNAL OF AUTOMOTIVE AND MECHANICAL ENGINEERING
ISSN: 2229-8649 e-ISSN: 2180-1606
VOL. 20, ISSUE 2, 2023, 10411 – 10421
DOI: https://doi.org/10.15282/ijame.20.2.2023.07.0805

RESEARCH ARTICLE

Influence of Heat Treatment on Microstructures and Shape Memory Effect of Cu-28Zn-2.5Al wt. % Produced by Gravity Casting

A. Setyani[1], I. A. Setiawan[2], P. R. Pamungkas[2], N. Sofyan[2] and B. T. Sofyan[2,3,*]

[1]Department of Metallurgical Engineering, Faculty of Mineral Technology, Universitas Pembangunan Nasional Veteran Yogyakarta, Kampus II Babarsari 2 Yogyakarta 55281, Indonesia
[2]Department of Metallurgical and Materials Engineering, Faculty of Engineering, Universitas Indonesia, Kampus UI Depok 16424, Indonesia
[3]Faculty of Defence Technology, Indonesia Defence University, Indonesia Peace and Security Center, Sentul, Bogor 16810, Indonesia

ABSTRACT - Cu-Zn-Al is one of the prospective shape memory alloys due to its promisingly good shape memory effect (*SME*), obtainable at a lower price through an easier fabrication process. Several hindrances that lower the *SME* of the Cu-Zn-Al can be improved by applying modified quenching methods and media. This study comprehensively studied the effects of quenching methods and media on Cu-28Zn- 2.5Al wt.% alloy. The alloy was fabricated by gravity casting and homogenized at 850 °C for 2 h. It was then betatized at 850 °C for 30 minutes and subsequently quenched using two different methods: direct quenching (DQ) and up quenching (UQ) with two different cooling media: water + dry ice (WD) and saltwater + dry ice (SD). Several characterizations to determine the material properties, such as morphology, structure, and hardness, were held, and additional semi-empirical bending tests were also conducted to determine the *SME* performance. The results showed that all quenched samples consisted of β' martensite [M18R] and retained α [A1] after quenching, regardless of the quenching method and cooling media. Upon analysis, the quenching with UQ method in SD media was found to be the most effective quenching process, as the method yields in an alloy with the highest *SME* performance. The pathway for achieving a high *SME* performance of Cu-Zn-Al alloy was thoroughly discussed in the article.

ARTICLE HISTORY
Received : 03rd Nov 2022
Revised : 07th June 2023
Accepted : 12th June 2023
Published : 30th June 2023

KEYWORDS
Shape memory alloy;
Shape memory effect;
Cu-Zn-Al;
Quenching method;
Quenching media

1.0 INTRODUCTION

Shape Memory Alloys (SMAs) are intelligent materials with the ability to deform and return to their pre-deformed shape after a short period of heating above the phase transformation temperature. The property of SMAs is formed through the formation of twinned martensite, a diffusionless transformation from the austenite to martensite phase by quenching with a rapid cooling rate. The capability of SMAs to return to their original shape is denoted as Shape Memory Effect (*SME*), which occurs due to thermoelastic transformation from the detwinned martensite phase to the austenite phase after heating and its subsequent transformation to its twinned form upon cooling [1]–[3].

The Cu-Zn-Al alloys are prospective SMAs to be researched as a substitute to Ni-Ti alloys because of their good shape recovery, at around ~5% better than Fe-based SMAs. Moreover, the Cu-Zn-Al also offers other benefits such as ease of fabrication, economical, high thermal conductivity as well as high electrical conductivity [1], [3], [4]. In Cu-Zn-Al alloys, the phase transformations from the austenite to the martensite can be summarized as follows: β [Body Centered Cubic]/[A2]→ [B2]→[[L21/ D03]→ [M18R], [9R], or [2H] depending on the alloying composition. The β [BCC] phase has an initial structure of A2, a disordered BCC phase. Upon cooling, the A2 transformed into a B2 superlattice through a nearest-neighbour ordering (nn) [5]–[8]. Further cooling then results in a next-nearest neighbor ordering (nnn), forming a D03 or L21 superlattice phase. The rapid cooling rate would cause an extra transformation step through a displacive transformation, in which the ordered phase may transform into either the martensitic phase of 18R, 9R, or 2H, depending on alloy composition [9]. Despite their prospects, the Cu-Zn-Al alloys SMA has several weaknesses, such as arguably low ductility, prone to room temperature ageing, and stable martensite phase [2],[10],[11]. Hence, the overall *SME* values are usually low.

These weaknesses have previously been mitigated by applying the Up Quenching (UQ) and Step Quenching (SQ) methods [7],[8],[12],[13]. Schofield and Miodownik [13] implemented the UQ (at 50 °C) to both Cu-25Zn-8.3Al and Cu-31.61Zn-4Al wt. %, and it successfully prevented martensite stabilization. Similarly, the UQ method was conducted on Cu-22Zn-4.6Al wt. % alloy by Longauer et al. [14] which display the capability to prevent martensite stabilization. The results suggest that the UQ method samples display *SME* characteristics, while the samples treated with direct quenching (DQ) and SQ treatment did not show any *SME* capabilities [14]. Another approach to prevent martensite stabilization was to apply alternative quenching media—research held by Spielfeld et al. [15] conducted liquid nitrogen quenching on the Cu-26.3Zn-3.9Al. The results suggest that quenching using media with low temperature (high cooling rate) could result

*CORRESPONDING AUTHOR | B.T. Sofyan | ✉ bondan@eng.ui.ac.id

in stable martensite due to lattice defects preventing the transformation to the austenite phase unless additional tempering treatment is given [15].

As previously discussed, both quenching methods and media play a key role in improving the *SME* capability of Cu-Zn-Al alloy. However, the effect of simultaneously changing both quenching methods and media is not well understood. In this research, a simultaneous study of both the effects of quenching methods and quenching media on the microstructures and *SME* properties of Cu-28Zn-2.5Al wt. % alloy was investigated. The mixture of dry ice and water (WD), as well as saltwater and dry ice (SD), which had lower temperatures (3 to -15 ℃) than water (25 ℃), was chosen, as it is lower than room temperature water although not as extremely cold as the liquid nitrogen (-196 ℃). These quenching media were also inexpensive and might be a promising alternative for industrial purposes. Meanwhile, the selection of alloy compositions with low Al content in the α+β phase region was selected to avoid excessive brittleness caused by the formation of too many β phase, which might hinder the machining process prior to heat treatment.

2.0 EXPERIMENTAL PROCEDURE

The Cu-28Zn-2.5Al wt. % was fabricated by gravity casting from pure metals. The Cu rods (99.5%, UD. Metallindo Sejahtera), Zn ingots (99.99%, Korea Zinc Co. Ltd.), and Al ingots (99%, PT. Inalum) were melted in a crucible at a temperature of 1150 ± 10 °C and casting process was subsequently held by pouring the melt into an AISI H-13 mould (110×110×6 mm^3). Preheating was held on the AISI H-13 mould prior to the casting process at a preheating temperature of 800 °C. After the casting process, the as-cast (AC) plate was homogenized at 850 ± 10 °C for 2h, followed by air cooling. Optical emission spectroscopy (OES) was used to characterize the nominal composition of the as-homogenized (A) sample, and the value are shown in Table 1.

Table 1. The nominal composition of the AH alloys

Element	Cu	Zn	Al	Fe	Pb	Mn	Ag	Cr	Sn	Co	Zr
wt. %	bal.	28.3	2.5	<0.005	<0.005	0.005	0.003	0.013	0.02	0.032	0.002

The AH plate was then cut into several plates with 50 × 20 × 6 mm^2 dimensions. The following cut plates were then betatized at a betatizing temperature (T_β) of 850 ± 10 °C for 30 min and then quenched using two different methods and two different quenching media. The details of the methods are as follows:

i. DQ_WD: quenching into water + dry ice bath (T_{bath1} = 2 °C) for 30 min.
ii. UQ_WD: quenching into water + dry ice bath (T_{bath1} = 2 °C) followed by quenching into boiling water bath (T_{bath2} = 100 °C) for 30 min and quenching in water + dry ice bath (T_{bath1} = 2 °C).
iii. DQ_SD: quenching into saltwater + dry ice bath (T_{bath1} = –15 °C) for 30 min.
iv. UQ_SD: quenching into saltwater + dry ice bath (T_{bath1} = –15 °C) followed by quenching into boiling water bath (T_{bath2} = 100 °C) for 30 min and quenching in saltwater + dry ice bath (T_{bath1} = –15 °C).

The schematic diagram of the quenching process of each method is shown in Figure 1.

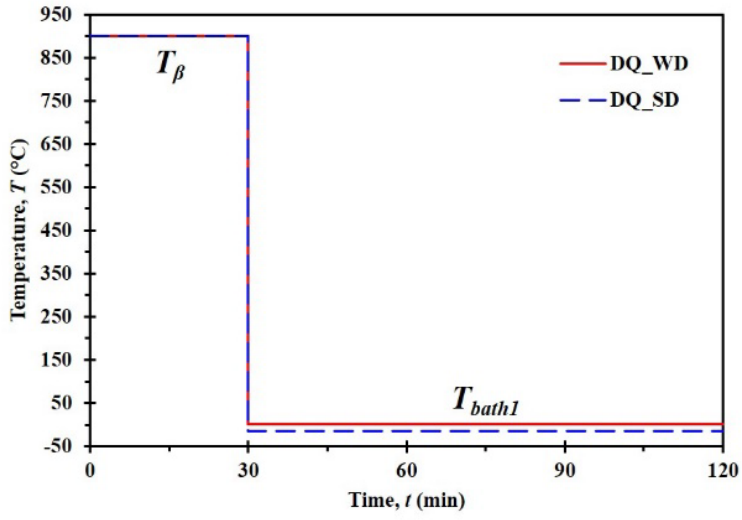

(a)

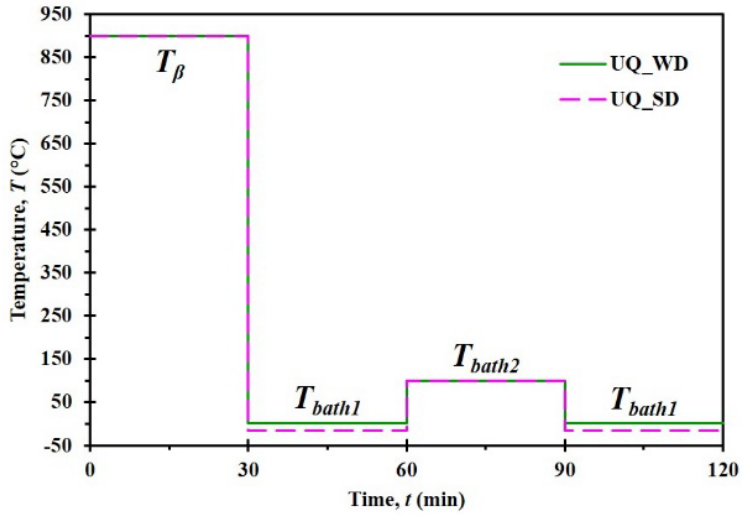

(b)

Figure 1. The schematic quenching process with (a) DQ and (b) UQ method using WD and SD quenching media

The microstructure observation was done using an optical microscope (OM, Zeiss Primotech) and scanning electron microscope/energy dispersive spectroscopy (SEM/EDS, FEI Inspect F50/Apollo X). The samples were prepared through the standard metallographic grinding and polishing process, followed by etching with $FeCl_3$ etchants (10-gram $FeCl_3$+95 mL alcohol 95%) for 5 s. Phase identification on samples was done by using x-ray diffraction (XRD, PAnalytical X'Pert Pro MPD) with Cu-Kα radiation. Following phase identification, the phase volume fractions were calculated using the ImageJ pixel counter. Prior to the counting, the OM images with 100× magnification were converted into black and white images to minimize the error calculation by using the thresholding function in Adobe Photoshop. The microhardness test was performed using the Vickers method in compliance with the ASTM E92 standard test procedure. Bending test preparation was conducted by cutting samples into a dimension of 5×0.4×0.1 cm using a diamond saw with a rotating speed (ω) of 300 rpm. A diamond saw-cutting tool is used to avoid excessive deformation of the as-quenched samples. Afterwards, each sample was manually bent with a rod (Ø = 20 mm). The bent sample was then dipped into a beaker with boiling water at 100 ºC for 5 minutes. The shape memory effect measurement was done by measuring the angle formed after the bending process (θ_s) and the final angle after dipping into boiling water at 100 ºC (θ_T). The measurement was conducted manually by tracing the formed angle on a piece of paper, followed by measuring the angle using a protractor. The semi-empirical bending process schematic can be seen in Figure 2.

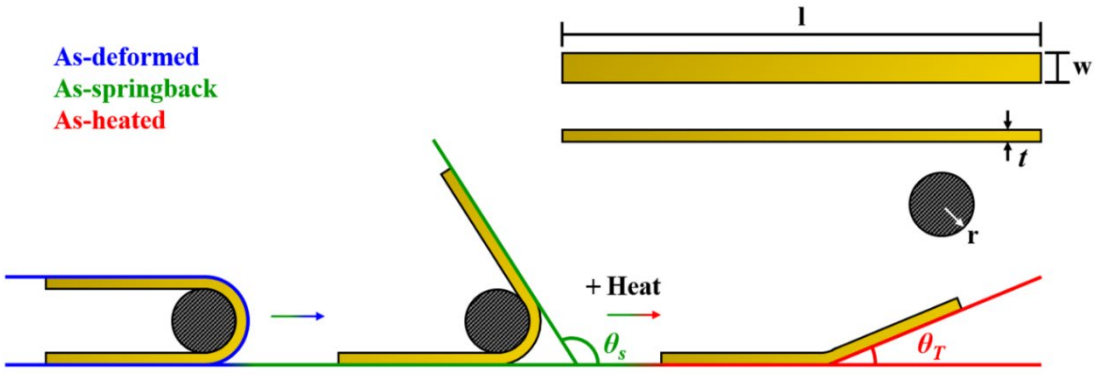

Figure 2. Schematic of bending test, rod radius (r) is 10 mm

3.0 RESULTS AND DISCUSSION

3.1 Microstructures and Phase Identification of AC and AH Alloys

The Cu-28Zn-2.5Al wt. % alloy microstructures in AC and AH conditions are shown in Figure 3. It is clear that Cu-28Zn-2.5Al wt. % alloy consists of two phases, which are the dark-colored phase as the matrix and the light-colored phase with lath morphology as the secondary phase. The AC and AH microstructures of Cu-28Zn-2.5Al wt.% alloy resemble the microstructures found by Stosic et al. [3] on Cu-25Zn-4Al wt. %, which also contained two phases, namely α dendritic phase spread over the β matrix. In addition, this microstructure also resembles the alloy fabricated by Setyani et al. [16], namely the α phase with lath morphology spread over the matrix in the form of a β phase. The SEM-EDS results on the AH samples in Table 2 show that the light-colored phase (points 2 and 3) contains 28.89-29.02 wt. % (Zn) and 1.32-1.42

wt. % (Al). Meanwhile, the dark-colored phase (point 1) has higher Zn and Al levels of 32.06 (Zn) and 1.74 (Al) wt. %, respectively. This result confirms that the dark phase with higher levels of Zn and Al is β phase with the Body-Centered Cubic (BCC) crystal structure, while the light phase with lower levels of Zn and Al is α phase with the FCC crystal structure. In addition, they are based on the plot on the isothermal section [17] of the Cu-28Zn-2.5Al wt. % alloy in the area of duplex phases, namely the α and β phases. In the solidification process of Cu-28Zn-2.5Al wt. %, the first phase formed is the β phase, followed by the formation of the secondary phase in the form of α phase. This also confirms that the phase formed in AC and AH is the β phase as matrix and the secondary phase is α with lath morphology. According to Sadayappan et al. [18], Al was able to promote the formation of the beta phase [BCC]. In shape memory alloy, the β phase becomes the parent phase (austenite) which then transforms into the martensite phase through a non-diffusion transformation mechanism when the alloy is quenched.

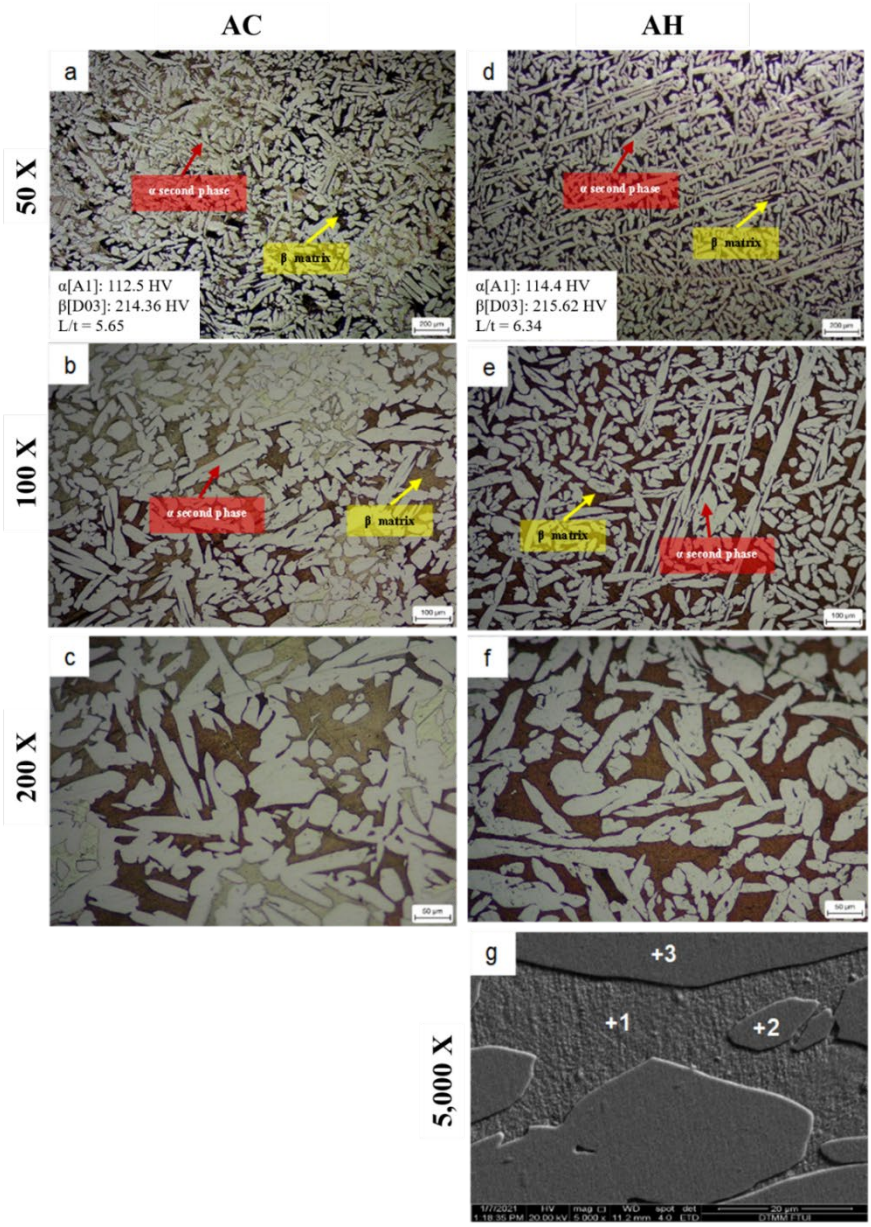

Figure 3. Microstructures of the AC (a) to (c) and AH (d) to (f) of Cu-28Zn-2.5Al wt. % alloy. Light-colored lath-shaped phase can be identified as α, while the dark-colored matrix phase can be identified as β. Picture (g) shows the SEM image of the as-homogenized Cu-28Zn-2.5Al wt. % alloy

Based on the quantitative test results, the volume fraction ratios of [α:β] Cu-28Zn-2.5Al wt. % in the AC and AH condition are [67:33] and [68:32], respectively. The volume fraction ratios are in line with the prediction using a tie line in the room temperature isothermal section of the Cu-Zn-Al system drawn by Liang et. al. [17]. The aspect ratio, indicated by the longitudinal divided by transversal length (L/t) ratio of the α phase in AC and AH are 5.65 and 6.34, respectively. As the secondary phase of α [FCC] has a lath morphology, the tip generally has an incoherent interface. The growth on the tip of the lath is more likely to occur because the incoherent interface does not have atomic interconnection [19]. As a result, this phase would tend to elongate than thicken. The post-homogenized composition has a higher aspect ratio than that of the AC.

Table 2. EDS microanalysis on the AH Cu-28Zn-2.5Al wt. %, spectra positions are shown in Figure 3(g)

Spectrum	Element (wt%)			Phase
	Cu	Zn	Al	
1	66.20	32.06	1.74	β [BCC]/[D03]
2	69.68	28.89	1.42	α [FCC]/[A1]
3	69.68	29.02	1.30	α [FCC]/[A1]

Figure. 4 shows diffractograms of Cu-28Zn-2.5Al wt.% composition in the AC and AH conditions. It could be seen that there are planes (1 2 2), (1 1 1), (2 0 0), and (2 2 0) indicating the presence of α phase [FCC] and (1 1 0), (2 1 1) peaks showing the β phase [BCC]. These planes matched well to the JCPDS Card No. 00-04-0836 (α) and 00-65-6066 (β). In addition, the peak formed is in line with the research held by Setyani et al. [16], where the appearance of peaks of 49.29°, 49.08°, 74.58° indicates the α phase peak. While the β phase is indicated by the presence of peaks of 42.39°, 76.58° and 43.46°. More detail of the 2θ position and miller indices (hkl value) of the XRD results can be seen in Table 3.

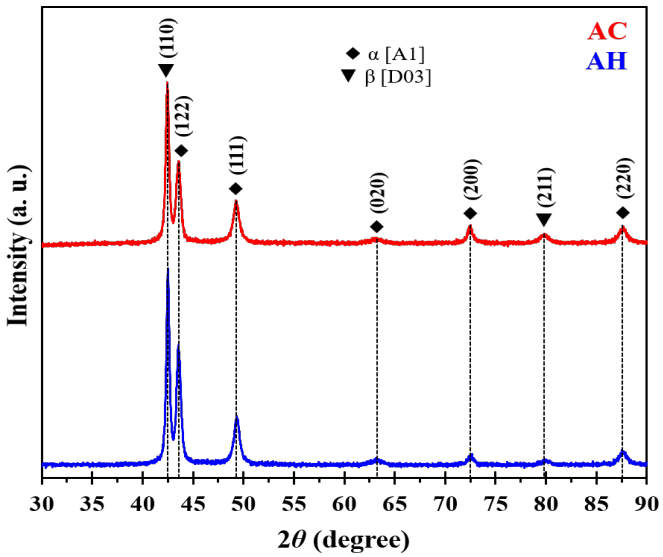

Figure 4. X-ray diffractograms of the AC and AH Cu-28Zn-2.5Al wt. % alloy

Table 3. The 2θ position and hkl of Cu-28Zn-2.5Al wt. % in the AC and AH conditions

Sample	2θ position	hkl	Phase
AC	43.51	(1 2 2)	α[FCC]/[A1]
	49.31	(1 1 1)	
	63.16	(0 2 0)	
	72.45	(2 0 0)	
	87.58	(2 2 0)	
	42.51	(1 1 0)	β[D03]
	80.01	(2 1 1)	
AH	43.53	(1 2 2)	α[FCC]/[A1]
	49.32	(1 1 1)	
	63.11	(0 2 0)	
	72.44	(2 0 0)	
	87.53	(2 2 0)	
	42.49	(1 1 0)	β[D03]
	79.96	(2 1 1)	

Aside from that, from the lattice parameters calculation on the AC samples, it is known that the α and β phases' lattice parameter values are a = 3.67 Å and a = 5.87 Å, respectively. Similarly, the lattice parameters of the α and β phases on the AH sample are 3.67 Å and 5.87 Å, respectively. Based on the EDX and XRD test results, it could be concluded that the AC and AH composition consist of two phases, which are the light phase as α (FCC), henceforth referred to as α [A1], and the dark-colored β phase [BCC], henceforth referred to as β [D03]. In addition, homogenization treatment on the AC sample did not cause a change in the crystal structure, whereas the α and β phases in AC and AH conditions had a cubic crystal structure.

The hardness test results are presented in Figure 5; it is clear that the β [D03] phase has higher hardness compared to the α [A1] phase. The hardness of the β [D03] phase on AC and AH conditions are 214.36 and 215.62 HVN, respectively. In contrast, the α phase hardness are 112.50 HVN in AC and 114.40 HVN in AH conditions. Furthermore, the AH treatment did not cause a significant change in hardness. This is in line with Setyani et al. [16] on the Cu-28Zn-3Al wt.

% alloy obtained a higher β phase hardness value than the α phase. In addition, Smirnov et al. [20] found the hardness in the alloy Cu-26Zn-5.27Al (α + β) binary composition, the hardness of the α phase was 130 – 146 HVN, while the hardness of the β phase was 200 – 275 HVN.

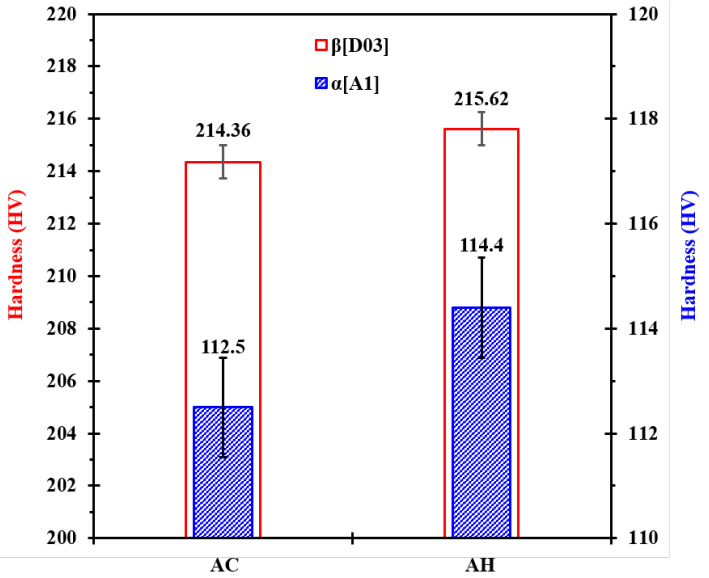

Figure 5. Microhardness values of α[A1] and β[D03] phase on the AC dan AH conditions of Cu-28Zn-2.5Al wt. % alloy

3.2 Effect of Quenching Method and Quenching Media on the Cu-28Zn-2.5Al wt. % SME Properties

The effect of quenching methods and quenching media on the Cu-28Zn-2.5Al wt.% alloy microstructures are shown in Figure. 6. As evidenced by the microstructure observation, the initial state in Figure 3(d) to 3(f), which consist of a duplex phase (α[A1] with lath morphology and β[D03] as matrix), had transformed into a phase with V-shaped twins as the matrix and the small-sized secondary phase. This V-shaped twins formed after quenching is morphologically similar to the previously obtained results by Lohan et al. [6] and Asanovic et al. on Cu-14.8Zn-5.8Al wt. % alloy. Asanovic et al. [21] on Cu-20.8Zn-5.8Al wt. % alloy identified as β′ [M18R] phase with monoclinic structure. In terms of morphology, the β' martensite structure has a particular characteristic of a V-shaped or needle-like shape. Meanwhile, the secondary phase was formed because the temperature of the homogenization process is too low; therefore prior to quenching, a small amount of α[A1] exists. The phase was then retained α, and as a result, the α[A1] phases were observed in all quenched samples.

Based on the quantitative measurement, the volume fraction of α[A1] in each sample is 23.15% (DQ_SD), 27.2% (DQ_WD), 29% (UQ_SD), and 30.5% (UQ_WD). There was an increase in the volume fraction of retained α[A1] in the UQ treatment, both while using WD and SD media. Asanovic et al. [21] had previously stated that UQ treatment could cause an increase in the volume fraction of either the secondary phase or the primary phase, which depends on the heating temperature and duration. If the sample is heated more than 180 ℃, precipitation of the γ phase would occur which subsequently increased the alloy's hardness [5], [10].

The EDS results that were displayed in Table. 4 shows that the secondary phase contains lower Zn and Al than the matrix, whether in DQ or UQ method using either WD or SD quenching media. The composition of Zn and Al in the secondary phase has an average of 28.3 and 1.5 wt. %, respectively. Meanwhile, the average content of the Zn and Al in the matrix is 30 and 2 wt. %, respectively. This indicates that the secondary phase is α [A1], which is then referred to as retained α[A1]. Meanwhile, the matrix is β' [M18R] with V shape morphology, similar to the β' phase as in Asanovic et al. [21], [22]and Lohan et al. [6].

Table 4. EDS microanalysis on the as-quenched Cu-28Zn-2.5Al wt. % alloy with variation quenching method and quenching media at positions shown in Figure. 6 (d, h, l, and p)

Sample	Point	Element (wt%)			Phase	Sample	Point	Element (wt%)			Phase
		Cu	Zn	Al				Cu	Zn	Al	
DQ_WD	1	69.06	29.40	1.54	α[FCC]/[A1]	DQ_SD	7	70.89	27.42	1.69	α[FCC]/[A1]
	2	69.62	28.83	1.55	α[FCC]/[A1]		8	70.73	28.14	1.13	α[FCC]/[A1]
	3	67.95	30.49	1.56	β'[M18R]		9	67.32	30.18	2.50	β'[M18R]
UQ_WD	4	69.71	28.34	1.95	α[FCC]/[A1]	UQ_SD	10	69.90	28.63	1.47	α[FCC]/[A1]
	5	69.20	28.72	2.08	β'[M18R]		11	70.62	28.21	1.17	α[FCC]/[A1]
	6	70.60	27.44	1.96	α[FCC]/[A1]		12	68.09	30.37	1.54	β'[M18R]

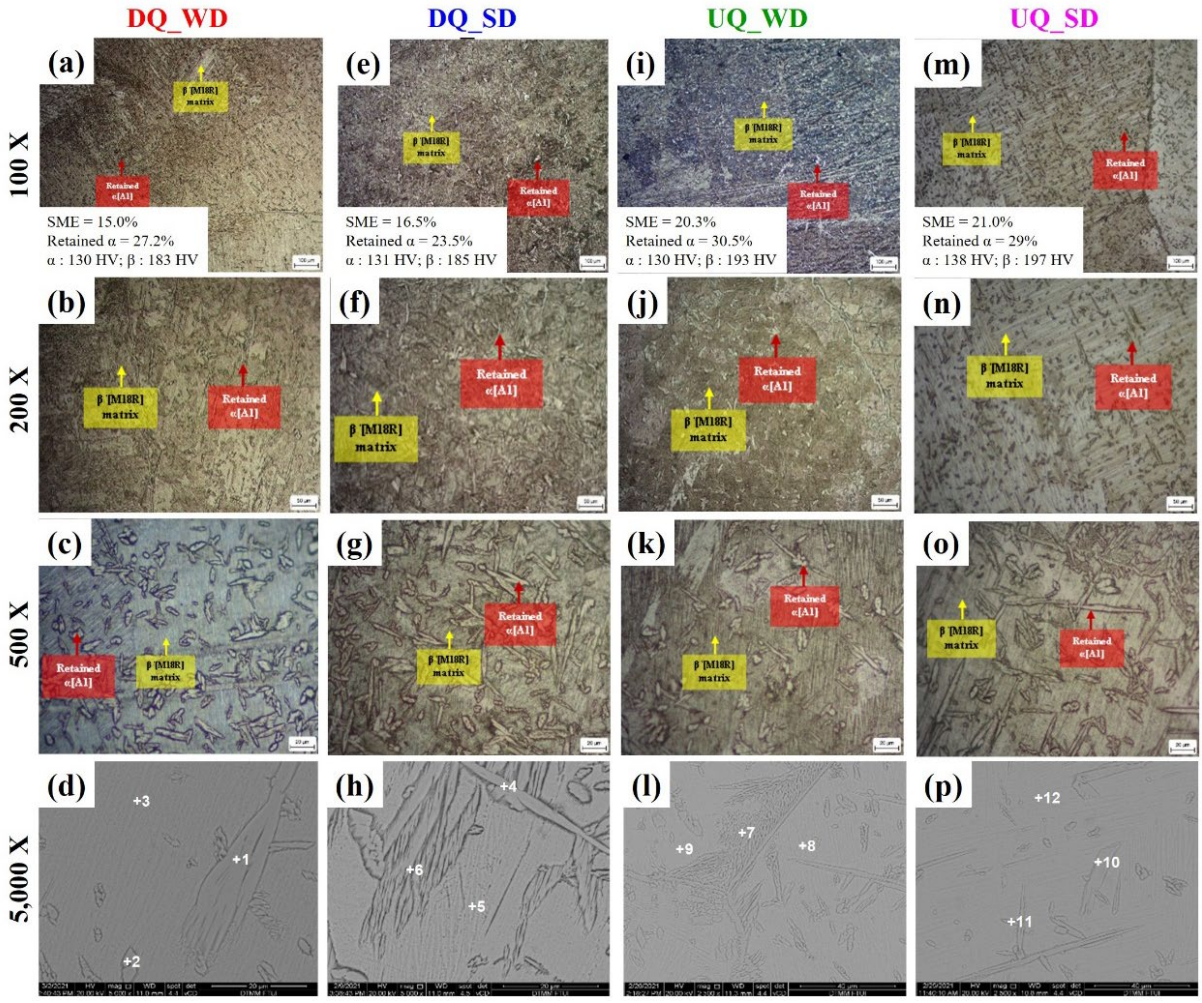

Figure 6. Microstructures of Cu-28Zn-2.5Al alloy with (a) to (d) DQ_WD, (e) to (h) UQ_WD, (i) to (l) DQ_SD, and (m) to (p) UQ_SD conditions (yellow arrows = β′[M18R] martensite phase in V shapes; red arrows = retained α)

The XRD test results are displayed in Figure 7 and Table 5. From the analysis of the XRD diffractograms, several peaks matched well with the positions related to the β′ phase [M18R], which corresponds to the (0 0 18), (2 0 2), (1 2 8), (3 2 0), (1 2 20), and (1 4 18) orientations [7]. Further, several other peaks were observed, which can be indexed as the (1 2 2), (2 0 0), and (2 2 0) planes of the α [A1] phase with FCC crystal structure. There was no significant peak shift due to the heat treatment of various quenching media and quenching methods. These results are in line with our previous research [16] on the alloy with a nominal composition of Cu-28Zn-3Al wt. % alloy, in which the variation of the quenching method, also yields in the martensite phase and retained α secondary phase. Moreover, these results are also in line with several other research conducted by Eskil et al. [7] on the Cu-24.9Zn-4.4Al wt alloy. % and Cu-21.6Zn-5.6Al wt.%, the two alloys were then treated with various quenching methods and quenching media consisting of DQ, UQ in water, and DQ, UQ in an oil bath. The results of the XRD test showed the same hkl with an insignificant change in the 2θ angle. Details of the 2θ position angle for DQ_WD, UQ_WD, DQ_SD, and UQ_SD methods are presented in Table 5.

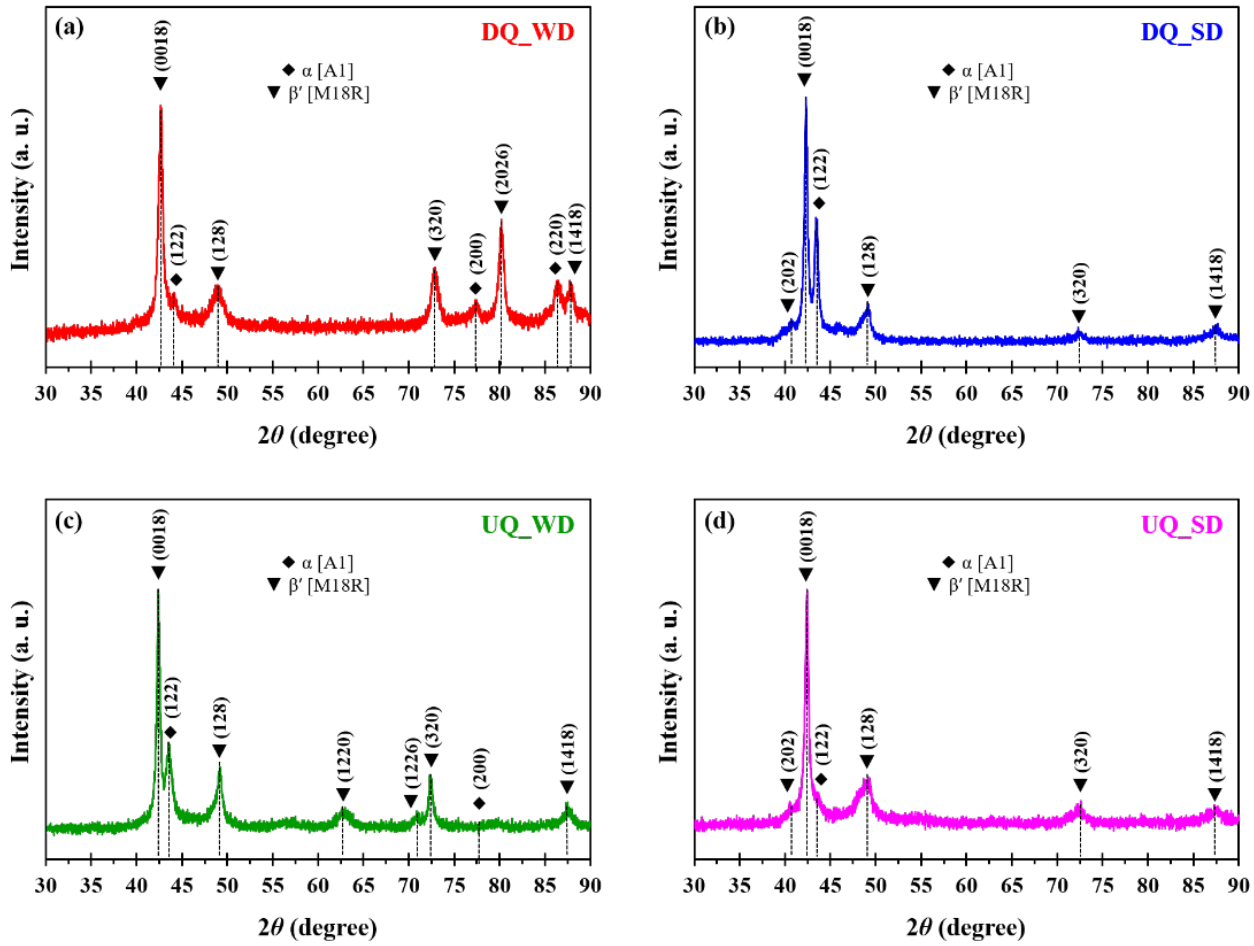

Figure 7. Diffractogram of Cu-28Zn-2.5Al alloy in (a) DQ_WD, (b) DQ_SD, (c) UQ_WD and (d) UQ_SD conditions. (WD: water + dry ice, SD: salt water+ dry ice)

Table 5. The 2θ position and hkl of Cu-28Zn-2.5Al wt. % alloy in DQ_WD, UQ_WD, DQ_SD and UQ_SD conditions

Phase	hkl	2θ position			
		DQ_WD	UQ_WD	DQ_SD	UQ_SD
α[FCC]/[A1]	(1 2 2)	44.30	43.74	43.41	43.61
	(2 0 0)	77.56	80.34	-	-
	(2 2 0)	86.70	-	-	-
β'[M18R]	(2 0 2)	-	-	40.64	40.69
	(0 0 18)	43.31	42.33	42.32	42.46
	(1 2 8)	49.06	49.31	49.21	49.12
	(1 2 20)	-	62.83	-	-
	(1 2 26)	-	70.96	-	-
	(3 2 0)	73.08	72.52	72.20	72.84
	(2 0 16)	79.96	-	-	-
	(2 0 26)	80.38	-	-	-
	(1 4 18)	87.42	87.97	87.43	87.66

From the microstructural observations, SEM-EDS, and XRD characterization on Cu-28.3Zn-2.5Al wt. % alloys with variations of quenching methods and quenching media confirmed that heat treatment caused the phase transformation, indicated by the formation of martensite β' phase as a matrix with V morphology. In addition, from the tests carried out, it is known that after quenching, retained α is formed with the FCC structure as the secondary phase which is spread over the matrix β′ martensite. This phenomenon is also similar to the results obtained by Stosic et al. [3] using Cu-25Zn-4Al wt.%, resulting in a martensite phase as matrix and retained α as the secondary phase after quenching using the SQ method. The application of UQ treatment of Cu-28Zn-2.5Al wt. % alloys caused an increase in the volume fraction of retained α but did not cause a new phase to appear.

The hardness test results on Cu-28Zn-2.5Al wt.% alloys after quenching are shown in Figure. 8. The hardness of UQ samples (UQ_WD and UQ_SD) is higher than that of DQ (DQ_WD and DQ_SD), although there is no significant difference. The alloys with quenching treatment using the UQ method have higher hardness due to the reheating treatment at 100 °C for 30 minutes, which helped to eliminate trapped vacancies due to the DQ quenching. The absence of a new

phase in UQ treatment causes the samples to have a similar hardness value. The γ phase in Cu-Zn-Al alloy will only appear if reheating exceeds 180 ℃ [14], [15]. In addition, the samples with SD media have higher hardness than that of WD media. This is due to the higher quenching rate caused by the SD media. Thus, the martensite phase is denser, and less retained α was formed. In SMA materials, the hardness value is expected not to reach too high value to avoid brittleness.

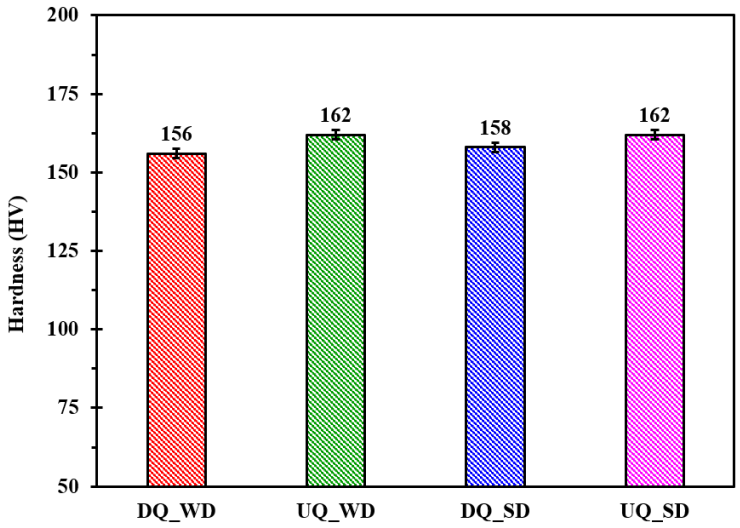

Figure 8. Microhardness comparison of DQ_WD, UQ_WD, DQ_SD and UQ_SD samples of Cu-28Zn-2.5Al wt. % alloy. (WD: water + dry ice, SD: salt water+ dry ice)

3.3 Shape Memory Properties of As-Quenched Cu-28Zn-2.5Al wt. % Alloy

The semi-empirical bending test result is shown in Figure. 9. It can be seen that the SME of the UQ method is better than the DQ method (UQ_SD: 21%, UQ_WD: 20.3%, DQ_SD: 16.5%, and DQ_WD:15%). The alloy quenched of salt water and dry ice mixture (SD) also yields a little bit better shape memory property as compared to the water + dry ice mixture (WD) counterpart. The UQ alloy *SME* is higher because the β′ phase in the UQ sample readily transforms into the β austenite phase as the heating applied during the UQ method eliminated the vacancies that caused the martensite stabilization. This argument is supported by research held by Gil et al. [23], which revealed the vacancies formed due to direct quench had obstructed the detwinning movement of the martensitic plates, hence, deteriorating the *SME*. Schofield and Miodownik [13] stated that the implementation of the UQ method on Cu-25Zn-8.3Al and Cu-31.61Zn-4Al wt.% could potentially hinder the formation of stable martensite, and thus *SME* can increase. Then, it can be concluded: that UQ treatment by using SD (saltwater + dry ice) is effective in increasing *SME*. In addition, Asanovic et al. [22] also mentioned that using the UQ method improved the ability to remember the shape of the alloy (*SME*) by preventing the formation of stable martensite. However, in this work, the increase in *SME* is not significant due to the relatively high retained α phase (23.5 - 30.5%). In developing SMA, aside from determining the appropriate treatment parameters, determining the composition of the alloy is also an important factor to consider, in order to obtain an alloy that is not brittle and produces a full martensitic phase after heat treatment.

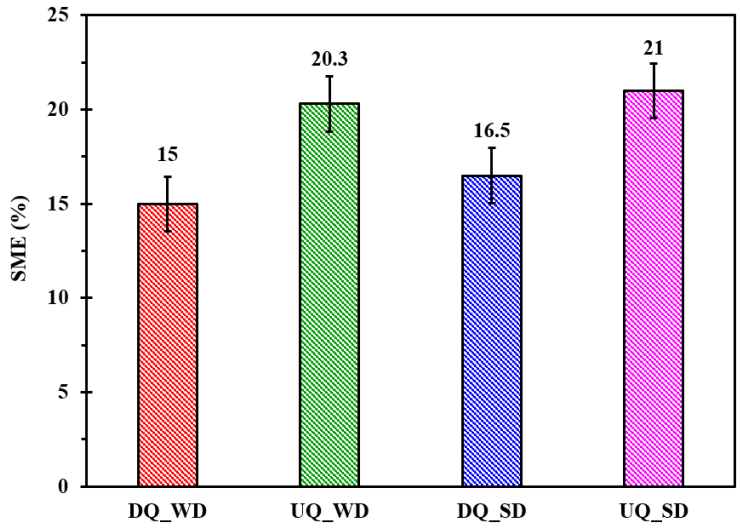

Figure 9. Shape memory effect (SME) of the Cu-28Zn-2.5Al wt. % after several different quenching methods and quenching media. (WD: water + dry ice, SD: salt water+ dry ice)

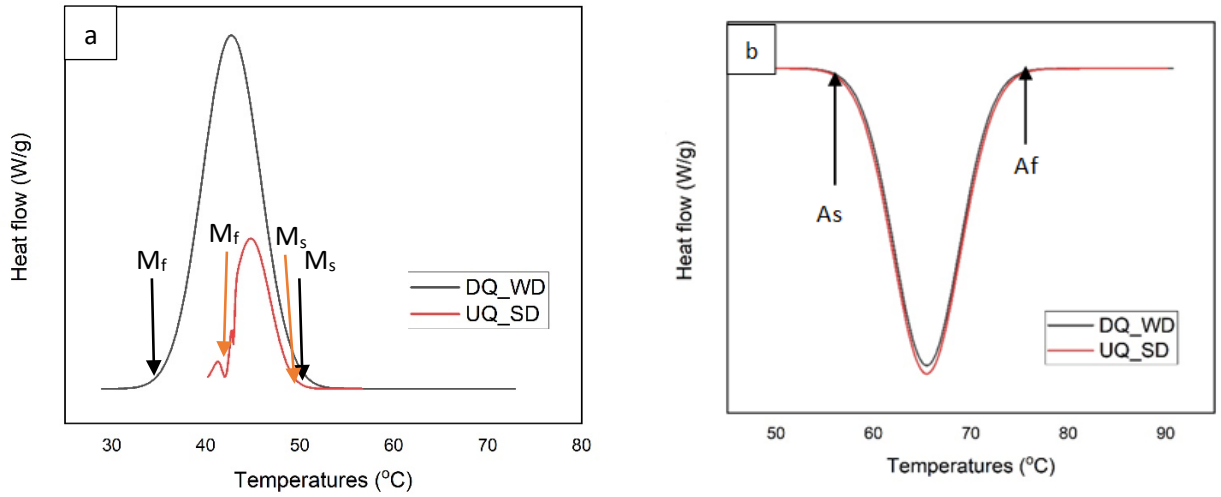

(a) (b)

Figure 10. Differential scanning calorimetry (DSC) curve in DQ_WD and UQ_SD samples of Cu-28Zn-2.5Al wt.% shape memory alloy (a) during cooling and (b) during heating

Table 6. Transformation temperature M_s, M_f, A_s, and A_f (°C) in DQ_WD and UQ_SD samples of Cu-28Zn-2.5Al wt. % shape memory alloy

Samples	Transformation temperature (°C)			
	M_s	M_f	A_s	A_f
DQ_WD	50	32	58.5	75
UQ_SD	49	40	58.0	75

Figure 10 and Table 6 show the test results of DSC testing. The test results show the cooling curve in Figure 10(a) and the heating curve in Figure 10(b) of the DQ_WD and UQ_SD samples. At the transformation temperature of austenite start (A_s) and austenite finish (A_f) the two samples showed almost the same temperature values. There is no significant difference. This is quite different from the exothermic curve seen in both samples, where the exothermic curve in the DQ_WD sample is higher, and the surface area is wider than of the UQ_SD sample. The values of M_s and M_f temperatures in the DQ_WD were 50 °C and 32 °C, while in UQ_SD samples are at 49 °C and 40 °C. In contrast, it was seen in the martensite finish temperature (M_f). Martensite finish means the final temperature for the formation of the β´ martensite phase. Through this transformation temperature data, it can be concluded that forming the martensite phase is easier for samples with SD media and UQ methods compared to DQ_WD samples because the M_f temperature of UQ_SD is higher than that of DQ_WD. The value of this transformation temperature is correlated with the ability to remember the shape of the alloy. *SME* test results are shown in Figure 9. The UQ_SD has a higher *SME* value of 21% which is 6% better compared to when the use of the DQ method with SD media with only 15% *SME*. The UQ quenching sample has a higher % recovery or *SME* compared to the DQ sample. The applied thermal energy during the UQ has caused the martensite phase to have better properties. The applied thermal energy during UQ helped the martensite to finish the ordering reaction, annihilate excess vacancy, as well as eliminate residual stresses due to quenching. Hence, the martensite stabilization is reduced, and the reverse phase transformation from martensite to austenite can be easily facilitated [13], [14], [22]. Other than quenching methods and quenching media in the development process of the shape memory alloy, it is necessary to look at the composition of the alloy and ratio of the phase contained in the alloy, as the initial characteristics of the material before treatment is defining the shape memory capability.

4.0 CONCLUSIONS

The effect of applying various heat treatments on microstructures and the *SME* of the Cu-28Zn-2.5Al wt.% alloy had been studied. Based on the finding and analysis conducted in the studies, it can be concluded as follows:

i. The AC and AH microstructure consists of binary phases; the dark-coloured matrix phase can be identified as the β [D03] phase, while the light-coloured and lath-shaped secondary phase can be identified as the α [A1] phase. The homogenization process increased the aspect ratio (L/t) of the α [A1] lath from 5.65 to 6.34. No substantial changes occur in both the hardness or the volume fraction of the alloy after homogenization.

ii. The heat treatment (DQ_WD, DQ_SD, UQ_WD, UQ_SD) process resulted in the formation of martensite phase β' [M18R] with V-shape twin as the matrix and uniformly dispersed retained α [A1] as the secondary phase. The volume fraction ratios of β' [M18R]: α [A1] of the samples (DQ _WD, DQ _SD, UQ _WD, and UQ_SD) are [98.4: 72.8], [76.5:23.5], [69.5:30.5], and [71:29], respectively.

iii. The strain recoveries of the DQ_WD, DQ_SD, UQ_WD, and UQ_SD are 15%, 16.5%, 20.3% and 21%, respectively. This indicates that UQ quenching method and using saltwater + dry ice as quenching media

produced better *SME* properties. This finding suggests that the UQ is substantially better than the DQ method, while using the SD quenching media slightly improves the *SME*.

iv. In developing the Cu-Zn-Al SMA, determining the composition of the alloy is also an important factor to consider aside from determining the appropriate treatment parameters, as a brittle martensite phase might be produced regardless of the heat treatment process due to the high nominal composition of the alloying elements.

v. The Ms, M_f, A_s, and A_f transformation temperatures on Cu-28Zn-2.5Al wt.% with DQ_WD treatments are 50, 32, 58.5, and 75 °C, respectively. While the M_s, M_f, A_s and A_f in UQ_SD there are 49, 40, 58, and 75 °C.

5.0 ACKNOWLEDGEMENT

This research was supported by PMDSU Research Grant from Kementerian Riset dan Teknologi/Badan Riset dan Inovasi Nasional Republik Indonesia with contract No: NKB-439/UN2.RST/HKP.05.00/2020.

6.0 REFERENCES

[1] K.K. Alaneme, and E.A. Okotete, "Reconciling viability and cost-effective shape memory alloy options – A review of copper and iron-based shape memory metallic systems," *Engineering Science and Technology an International Journal*, vol. 19, no. 3, pp. 1582–1592, 2016.

[2] C.M. Wayman, and T.W. Duerig, "An introduction to martensite and shape memory," In *Engineering aspects of shape memory alloys*, Duerigh, Ed. UK: Butterworth-Heinemann, pp. 3–20, 1990.

[3] Z. Stošić, D. Manasijevica, L. Balanovica, T.H. Grguricb, U. Stamenkovica, et al., "Effects of composition and thermal treatment of Cu-Al-Zn alloys with low content of Al on their shape-memory properties," *Journal of Materials Research*, vol. 20, no. 5, pp. 1425–1431, 2017.

[4] R. Dasgupta, A.K. Jain, P. Kumar, S. Hussein, and A. Pandey, "Effect of alloying constituents on the martensitic phase formation in some Cu-based SMAs," *Journal of Materials Research and Technology*, vol. 3, no. 3, pp. 264–273, 2014.

[5] M.H. Wu, *Cu-Based Shape Memory Alloys. Engineering aspects of shape memory alloys*, UK: Butterworth-Heinemann Ltd, pp. 69-88, 1990.

[6] N.M. Lohan, M.G. Suru, B. Pricop, and L.G. Bujoreanu, "Cooling rate effects on the structure and transformation behavior of Cu-Zn-Al shape memory alloys," *International Journal of Minerals, Metallurgy and Materials*, vol. 21, no. 11, pp. 1109–1114, 2014.

[7] M. Eskil, and N. Kayali, "X-ray analysis of some shape memory CuZnAl alloys due to the cooling rate effect," *Materials Letters*, vol. 60, no. 5, pp. 630–634, 2006.

[8] P.S. Lobo, J. Almeida, and L. Guerreiro, "Shape memory alloys behaviour: A review," *Procedia Engineering*, vol. 114, pp. 776–783, 2015.

[9] A. Cuniberti, R. Romero, and A. Condó, "Compression-induced hexagonal martensite in Cu-Zn-Al," *Materials Science and Engineering A*, vol. 325, no. 1–2, pp. 177–181, 2002.

[10] M. Blanco, J.T.C. Barragan, N. Barelli, R.D. Noce, C.S. Fugivara et al., "On the electrochemical behavior of Cu-16%Zn-6.5%Al alloy containing the β'-phase (martensite) in borate buffer," *Electrochim Acta*, vol. 107, pp. 238–247, 2013.

[11] X. Cheng, F. Huang, N. Li, and X. Wu, "Microstructure and shape memory effect of Cu-26.1Zn-4.8Al alloy," *Journal of Wuhan University of Technology Materials Science Edition*, vol. 23, no. 5, pp. 717–719, 2008.

[12] K. Prakash, and V.R. Harchekar, "Optimization of rebetatising time and temperature for lowering martensitic transformation temperature in Cu-Zn-4% Al shape memory alloy," *Indian Journal of Engineering and Materials Sciences*, vol. 4, pp. 67–70, 1997.

[13] D. Schofield, and AP. Miodownik, "Aging effects in copper-based shape-memory alloys," *Metals and Technology*, vol. 7, pp. 167–173, 1980.

[14] S. Longauer, M. Votjko, G. Janak, and M. Longauerova, "Stabilization of martensite in also microstructure of a Cu-Zn-AI shape-memory alloy," *Journal de Physique IV France*, vol. 112, pp. 523–527, 2003.

[15] J. Spielfeld, "Marforming and martempering of a Cu-Zn-Al shape memory alloy," *Materials Science and Engineering: A*, vol. 273–275, pp. 639–643, 1999.

[16] A. Setyani, I.A. Setiawan, D.R.K. Pertiwi, and B.T. Sofyan, "Effects of quenching methods on shape memory properties of Cu-28Zn-3Al wt. % alloy produced by gravity casting," *Indian Journal of Engineering & Materials Sciences*, vol. 29, pp. 100-107, 2022.

[17] S-M. Liang, and S-F. Rainer, *CALPHAD: Computer coupling of phase diagrams and thermochemistry thermodynamic assessment of the Al – Cu – Zn system, Part III: Al – Cu – Zn ternary system*. Calphad, 2016; 52: pp. 21–37.

[18] M. Sadayappan, J.P. Thomson, M. Elboujdaini, and P.G. Gu, Grain refinement of permanent mold cast copper base alloys, Copper Development Association, New York, 2005.

[19] D.A. Porter, and K.E. Easterling, *Phase transformations in metals and alloys*. UK: Typesetter Ltd, 1992.

[20] S.V. Smirnov, M.V. Myasnikova, and N.B. Pugacheva, "Hierarchical simulation of plastic deformation and fracture of complexly alloyed brass," *International Journal of Damage Mechanics*, vol. 25, pp. 251–265, 2016.

[21] V. Asanović, K. Delijić, and N. Jauković, "A study of transformations of β-phase in Cu-Zn-Al shape memory alloys," *Scripta Materialia*, vol. 58, pp. 599–601, 2008.

[22] V. Asanovic, D. Radonjic, J. Scepanovic, and D. Vuksanovic, "Effect of chemical composition and quenching media on recoverable strain in Cu-Zn-Al alloys," *Journal of Materials Research and Technology*, vol. 12, pp. 1368-1379, 2021.

[23] F.J. Gil, and J.M. Guilemany, "The determination of the influence of heat treatment on the martensitic transformation in Cu-Zn-Al-Mn shape-memory alloy by calorimetry and acoustic emission techniques," *Thermochimica Acta*, vol. 205, pp. 75–85, 1992.